# Effects of a Vertical Shaft to Muon Background

Alfred Tang

Chinese University of Hong Kong
Physics Department, Shatin, New Territories, Hong Kong

Email: atang@phy.cuhk.edu.hk

September 6, 2005

**Abstract**

The effects of a vertical shaft on the muon background of an underground detector are analyzed using `MUSIC`.

## 1 Introduction

It is usually assumed that the vertical shaft does not contribute to the muon background significantly. Since the sealevel muon distribution is mostly vertical, it is possible that the vertical shaft has some effects on the muon background if the detector is placed sufficiently close to it. This report analyzes the effects of the shaft on muon background. In this analysis, muon energy and flux from a flat surface is calculated with `MUSIC` by subtracting the path lengths of the muons inside the shaft vloume. A detailed calculation should also substract the volume of the detector hall from the simulation. The present preliminary calculation does not attend to this level of detail but takes the simplifying assumptions that the detector hall volume is zero and that the detector is a mathematical point.

## 2 Modified Gaisser Parameterization

The accuracy of the simulation depends on `MUSIC`, the parameterization of the surface muon intensity and the user-supplied sampling algorithm. A standard atmospheric muon parameterization is given by Gaisser [1] as

$$\frac{dN_{\mu 0}}{dE_{\mu 0} d\Omega} \simeq A \frac{0.14 E_{\mu 0}^{-2.7}}{\text{cm}^2 \text{ sr s GeV}} \left\{ \frac{1}{1 + \frac{1.1 \tilde{E}_{\mu 0} \cos\theta}{115}} + \frac{.054}{1 + \frac{1.1 \tilde{E}_{\mu 0} \cos\theta}{850}} + r_c \right\}. \tag{1}$$

The original Gaisser parameterization has $A = 1$, $E_{\mu 0} = \tilde{E}_{\mu 0}$ and $r_c = 0$. Muon energy $E_{\mu 0}$ at the surface is measured in GeV and $\theta$ is the zenith angle. The differentials of time $dt$ and area $dS$ are omitted from the denominator on the left-hand-side of Eq. (1) for the sake of simplicity. The standard Gaisser parameterization in Eq. (1) has the correct angular behavior of $\sec\theta$ at high energy $E \geq 100/\cos\theta$GeV and small angle $\theta < 70^\circ$ where the effect due to the curvature of the earth is negligible. In the low energy limit ($E_{\mu 0} \leq 100/\cos\theta$ GeV), the Gaisser parameterization is significantly higher than the observed values. The expected angular dependence of $\cos^n\theta$ with $n \sim 2$ in this regime must also be taken into account. For these reasons, the following modifications [3] to Eq. (1) are suggested:

$$r_c = 10^{-4}, \tag{2}$$

$$\Delta = 2.06 \times 10^{-3} \left( \frac{950}{\cos\theta^\star} - 90 \right), \tag{3}$$

$$\tilde{E}_{\mu 0} = E_{\mu 0} + \Delta, \tag{4}$$

$$A = 1.1 \left( \frac{9\sqrt{\cos\theta + 0.001}}{103} \right)^{\frac{4.5}{E_{\mu 0} \cos\theta^\star}}. \tag{5}$$

It is important to note the term involving $\cos\theta$ inside the square root of Eq. (5) does not have a star. For very low muon energy ($E_{\mu 0} \leq 1/\cos\theta$ GeV), the substitution

$$E_{\mu 0} \rightarrow \frac{3E_{\mu 0} + 7\sec\theta^\star}{10} \tag{6}$$

is made before $E_{\mu 0}$ is passed to Eqs. (1)–(5). Figure 1 illustrates the new fits due to the changes made in Eqs. (2)–(6) for several zenith angles. Eq. (5) has the appearance of danger when $\cos\theta \rightarrow 0$. As it turns out, $\cos\theta$ will be replaced by $\cos\theta^\star \geq 0.103458$ so that stack overflow will not be a problem. The zenith angle on top of the atmosphere $\theta^\star$ is not the same as the zenith angle $\cos\theta$ at depth $h$ due to the curvature of the earth. However the former can be parameterized in terms of the latter as [4]

$$\cos\theta^\star = \sqrt{\frac{x^2 + p_1^2 + p_2 x^{p_3} + p_4 x^{p_5}}{1 + p_1^2 + p_2 + p_4}}, \tag{7}$$

where $x \equiv \cos\theta$, $p_1 = 0.102573$, $p_2 = -0.068287$, $p_3 = 0.958633$, $p_4 = 0.0407253$ and $p_5 = 0.817285$. The terms involving $\cos\theta$ in Eq. (1) must be replaced by $\cos\theta^\star$ if large angles ($\theta > 70°$) are used in the calculations.

# 3 Subtraction Scheme

Figure 2 illustrates the geometry of the vertical shaft and the point-like detector. The muon ray intersects the wall of the shaft at two points in this illustration. The radius and the depth of the shaft are $r$ and $h$ respectively. Assuming that the point-like detector lies on a plane containing the bottom of the shaft, the vertical depth of the detector is also $h$. The distance between the detector and the principle axis of the shaft is labeled as $\rho$. When the muon does not intersect the shaft, the depth $X$ (distance between the flat surface and the detector traveled by the muon) is simply

$$X = \frac{h}{\cos\theta} \tag{8}$$

where $\theta$ is the zenith angle subtended at the detector. If the muon ray intersects the shaft, the distance traveled by the muon inside the shaft volume has to be subtracted before it is passed to `MUSIC`. The path lengths of the muon between the detector and the points of intersection with the wall of the shaft are $x1$ and $x2$ with $x2 > x1$. In the case of the muon passing through the shaft, the depth is calculated as

$$X = \frac{h}{\cos\theta} - \frac{2\rho}{\sin\theta}\sqrt{\cos^2\phi' + \left(\frac{r}{\rho}\right)^2 - 1} \tag{9}$$

for $x2 < h/\cos\theta$ and $\phi' < \sin^{-1}(r/\rho)$, or

$$X = \frac{\rho}{\sin\theta}\left(\cos\phi' - \sqrt{\cos^2\phi' + \left(\frac{r}{\rho}\right)^2 - 1}\right) \tag{10}$$

for $x1 < h/\cos\theta < x2$ and $\phi' < \sin^{-1}(r/\rho)$. The symbol $\phi'$ in Eqs. (9)–(10) is defined as $\phi' \equiv |\phi - \phi_0|$ where $\phi_0$ specifies the direction of the shaft with respect to the detector. The effects of shaft disappear in the limit of $\rho \rightarrow \infty$.

# 4 Results

Table 1 shows the dependence of muon energy and flux on the detector-shaft separation $\rho$ in the case of a shaft with the radius 5 m. In the present simulation, the detector is point-like and the volume of the detector is assumed to be zero. The simulations suggest that the effects of the shaft on muon background is negligible as long as the detector is placed at a small distance from the shaft. The final simulation should include the consideration of the sizes of the detector and the experimental hall whenever the relevant parameters are made available.

# References


[1] T. K. Gaisser and T. Stanev, "Cosmic Rays," Review of Particle Physics, edited by L. Alvarez-Gaumé *et al.*, Physics Letters, **B**592, 228 (2004).

[2] P. J. Hayman and A. W. Wolfendale, Proc. Phys. Soc. **80**, 710 (1962).

[3] The original form of the modifications to the Gaisser parameterization at low energy was suggested by V. A. Kudryavtsev in a private email which was later improved by A. Tang.

[4] D. Chirkin, `hep-ph/0407078`.

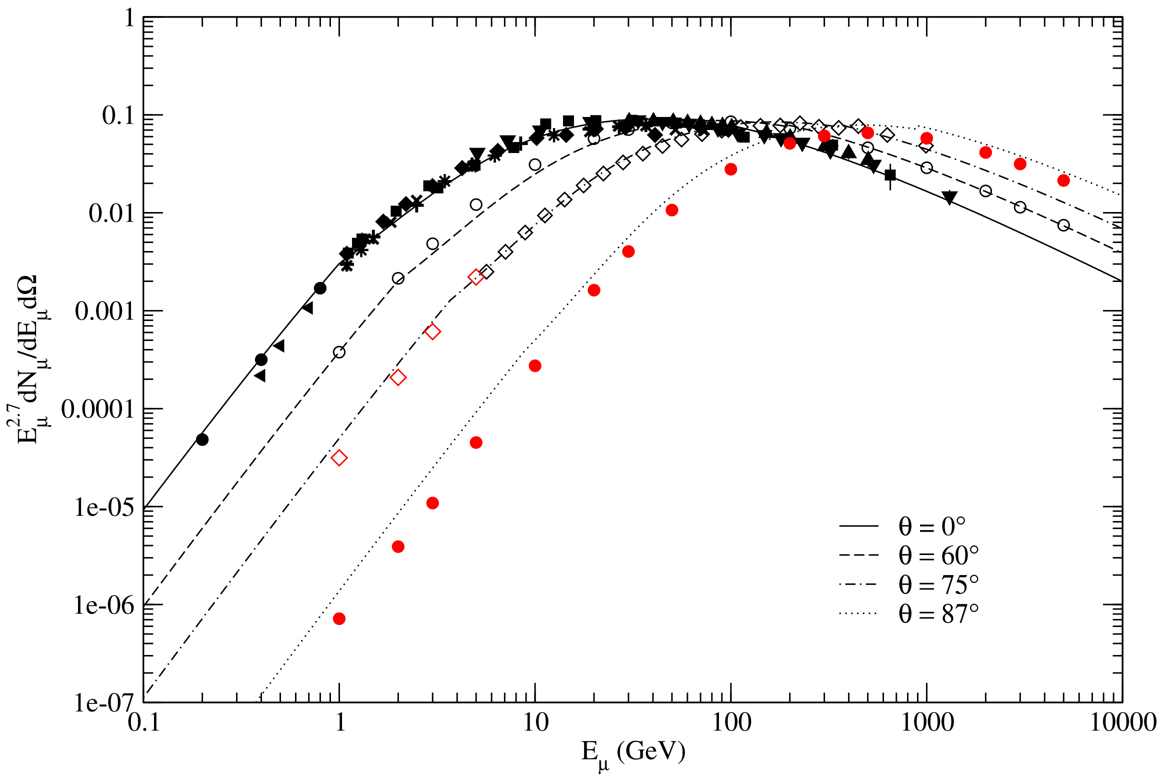


Figure 1: Fits of the modified Gaisser parameterization to experimental data in the low energy regime between $\theta = 0$ and $\theta = 87°$. The experimental data are taken from references [1]–[2]. The modified Gaisser parameterization is given by Eqs. (1)–(7).

Table 1: Comparison of integrated muon energy $E_\mu$ and flux $J_\mu$ at various distance $\rho$ between the principle axis of the vertical shaft and the point-like detector at 464 mwe. The radius of the shaft is 5 m.

| $\rho$ (m) | $E_\mu$ (GeV) | $J_\mu$ ($10^{-5}$ cm$^{-2}$ s$^{-1}$) |
|---|---|---|
| 0 | 41.2 | 5.39 |
| 10 | 88.8 | 2.22 |
| 20 | 91.2 | 2.12 |
| 30 | 91.8 | 2.09 |
| 40 | 91.9 | 2.08 |
| 50 | 91.3 | 2.10 |
| 60 | 91.3 | 2.10 |
| 70 | 91.4 | 2.10 |
| 80 | 91.7 | 2.09 |
| 90 | 91.4 | 2.10 |
| 100 | 91.4 | 2.10 |
| $\infty$ | 91.9 | 2.08 |

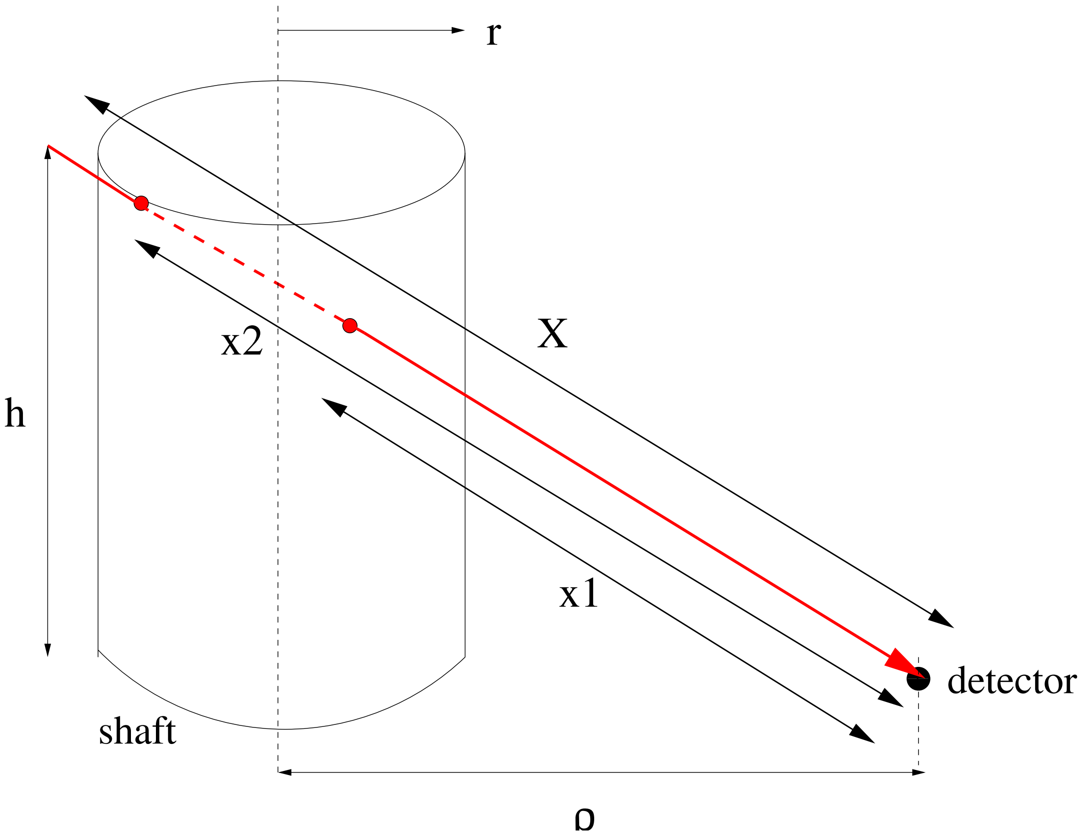


Figure 2: A sketch of the geometry of the vertical shaft, a muon ray (in red) and the point-like detector (represented by the black dot). The two red dots represent the points of intersection between the muon ray and the wall of the shaft.